

# A magnetoelastic resonance biosensor immobilized with polyclonal antibody for the detection of *Salmonella typhimurium*

R. Guntupalli<sup>a</sup>, J. Hu<sup>a,d</sup>, Ramji S. Lakshmanan<sup>a</sup>, T.S. Huang<sup>b</sup>,  
James M. Barbaree<sup>c</sup>, Bryan A. Chin<sup>a,\*</sup>

<sup>a</sup> Materials Research and Education center, Auburn University, Auburn, AL 36849, USA

<sup>b</sup> Department of Nutrition and Food Science, Auburn University, Auburn, AL 36849, USA

<sup>c</sup> Department of Biological Sciences, Auburn University, 101 Life Sciences Bldg., Auburn, AL 36849, USA

<sup>d</sup> Department of Material Science and Engineering, Jiangsu Polytechnic University, Changzhou 213016, PR China

Received 16 April 2006; received in revised form 27 June 2006; accepted 30 June 2006

Available online 22 August 2006

## Abstract

Mass-sensitive, magnetoelastic resonance sensors have a characteristic resonant frequency that can be determined by monitoring the magnetic flux emitted by the sensor in response to an applied, time varying, magnetic field. This magnetostrictive platform has a unique advantage over conventional sensor platforms in that measurement is wireless and remote. A biosensor for the detection of *Salmonella typhimurium* was constructed by immobilizing a polyclonal antibody (the bio-molecular recognition element) onto the surface of a magnetostrictive platform. The biosensor was then exposed to solutions containing *S. typhimurium* bacteria. Binding between the antibody and antigen (bacteria) occurred and the additional mass of the bound bacteria caused a shift in the sensor's resonant frequency. Sensors with different physical dimensions were exposed to different concentrations of *S. typhimurium* ranging from  $10^2$  to  $10^9$  CFU/ml. Detection limits of  $5 \times 10^3$  CFU/ml,  $10^5$  CFU/ml and  $10^7$  CFU/ml were obtained for sensors with the size of  $2 \text{ mm} \times 0.4 \text{ mm} \times 15 \text{ }\mu\text{m}$ ,  $5 \text{ mm} \times 1 \text{ mm} \times 15 \text{ }\mu\text{m}$  and  $25 \text{ mm} \times 5 \text{ mm} \times 15 \text{ }\mu\text{m}$ , respectively. Good agreement between the measured number of bound bacterial cells (as measured by scanning electron microscopy (SEM)) and frequency shifts was obtained.

© 2006 Elsevier B.V. All rights reserved.

**Keywords:** Magnetoelastic; Magnetostrictive; Biosensor; Antibody; *Salmonella typhimurium*; Langmuir Blodgett

## 1. Introduction

Foodborne pathogens have been found to cause food contamination at every stage of food production, processing, and distribution. *Salmonella typhimurium* is a gram-negative food pathogen that affects the abdomen causing infection, diarrhea and pain (CNIE, 2005). One of the common sources of *Salmonella* is contaminated poultry products (Gay, 1999). It is desirable to investigate rapid, sensitive, selective and real-time detection technologies for the identification of contaminated food products.

Various monitoring techniques have been developed to detect foodborne pathogens (Rogers, 2006). Conventional detec-

tion methods, such as enzyme-linked immunosorbent assay (ELISA), have been developed to detect pathogens in food products but require time-consuming pre-enrichment steps (Beckers et al., 1998; Hayes et al., 1991). The polymerase chain reaction (PCR) technology has become the gold standard for the detection of pathogens in food (Karpiskova et al., 2000; Luk, 1994; Oliveira et al., 2002). However dot-blot hybridizations which are used to prove the presence of specifically amplified products require multi-step processing and thus add considerable time and expense to the detection (Oberst et al., 1998).

Existing biosensor technologies such as surface acoustic wave (SAW) devices (Howe and Harding, 2000), quartz crystal microbalance (QCM) based immunosensors (Olsen et al., 2003; Olsen et al., 2006; Su and Li, 2005; Bandey et al., 2004 and Bailey, 2003) and optical fiber devices (Tims and Lim, 2004; Ko and Grant, 2006) offer very good performance in terms of

\* Corresponding author. Tel.: +1 334 844 3322; fax: +1 334 844 3400.

E-mail address: [bchin@eng.auburn.edu](mailto:bchin@eng.auburn.edu) (B.A. Chin).

sensitivity. However, the need for direct physical contacts (electrical wiring) places a constraint on the use of these sensors in real time applications such as detection in conducting liquids or sealed and opaque containers, and biological experiments such as the monitoring of bloodstream chemistry. The goal of our research is to develop a biosensor that can be used for remote and real-time sensing of pathogens in food products.

Magnetostrictive materials are made of amorphous ferromagnetic alloys composed of iron, nickel, molybdenum and boron. Due to the magnetoelastic nature of the amorphous magnetostrictive alloy, it exhibits a physical resonance when it is exposed to a time-varying magnetic field. This resonance can be monitored by using a pickup coil without the use of direct physical connections. Because of this unique advantage, numerous magnetostrictive materials applications have been proposed, including the detection of pH, humidity, temperature, viscosity, and stress etc. (Grimes et al., 2000; Cai et al., 2001; Jain et al., 2000; Kouzoudis and Grimes, 2000; Plamen et al., 2000; and Ong et al., 2001).

This paper presents the results of an investigation into a biosensor consisting of a magnetostrictive platform immobilized with a polyclonal antibody (the bio-molecular recognition element) for the detection of *S. typhimurium*.

## 2. Materials and methods

### 2.1. Sensor platform

METGLAS<sup>®</sup> 2826MB alloy (Conway, SC) obtained from Honeywell International was used as the sensor platform. The composition is Fe<sub>40</sub>Ni<sub>38</sub>Mo<sub>4</sub>B<sub>18</sub> and its theoretical value of the saturation magnetostriction is 12 ppm. To increase the mass sensitivity, sensors were mechanically polished using fine grit paper to reduce the thickness from 30 to 15 μm to decrease the initial mass. Magnetostrictive strips were made using an auto controlled, micro dicing saw. The diced sensors were ultrasonically cleaned in methanol solution to remove grease and debris left by the dicing process. To improve the environmental stability as well as bioactivity of the biosensors, thin layers of chromium and gold were coated onto the surfaces of the magnetostrictive particles using a Denton<sup>™</sup> (Moorestown, NJ) high vacuum RF sputtering system.

### 2.2. Antibodies and *Salmonella typhimurium* cultures

Rabbit polyclonal antibody (1 mg/ml) to *S. typhimurium* was purchased from Abcam Inc (Cambridge, MA) and immobilized onto magnetostrictive biosensors using the Langmuir–Blodgett (LB) film technique. The functional performance of the biosensors was evaluated with bacterial suspensions. *S. typhimurium* (ATCC 13311) obtained from the American Type Culture Collection (Rockville, MD) was confirmed for identity and propagated in the Department of Biological Sciences at Auburn University. The suspension was serially diluted with water to prepare bacterial suspensions ranging from 10<sup>2</sup> to 10<sup>9</sup> CFU/ml. All test solutions were prepared the same day as biosensor testing and maintained at 4 °C.

### 2.3. Monolayer deposition

The Langmuir Blodgett (LB) technique was used to immobilize the antibody onto the magnetoelastic resonance sensors. Antibody monolayers were deposited onto the sensor surface using a LB film balance KSV 2200 LB (KSV Chemicals, Finland). This system consists of a Wilhelmy-type surface balance (Sensitivity range 0–100 mN/m), a teflon trough of dimensions 45 cm × 15 cm, and a teflon barrier (0–200 mm/min) driven by a variable speed motor, all of which are encased in a laminar flow hood. To minimize variations that may arise due to vibrations, the trough is mounted on a marble table and aided by interposing rubber shock absorbers. The subphase temperature (20 ± 0.1 °C) control is achieved by circulating water through a quartz tube coil at the bottom of the trough. The magnetoelastic resonance sensors were submerged into the deionized water (DD H<sub>2</sub>O) in the LB trough. A monolayer from the antibody suspension was formed by allowing 100 μl of antibody solution (1 mg/ml) to run down a wetted glass rod that was partially submerged into the subphase (deionized water). When the antibody solution reaches the air–water interface, it splits into a monolayer due to surface forces (Pathirana et al., 2000). After spreading, the monolayer was allowed to equilibrate and stabilize for 10 min at 19 °C.

Monolayers were then compressed using a computer controlled compression barrier at a rate of 30 mm/min, until the pressure reached 22 mN/m. After reaching 22 mN/m pressure, the pressure was held constant and vertical antibody film deposition was carried out at a rate of 4.5 mm/min. Multiple monolayers of antibody were obtained by successive dipping the sensors through the monomolecular film deposited at a water–air interface. Seven monolayers containing antibodies were transferred onto the magnetostrictive sensor surface. Only one surface of the magnetostrictive sensor was coated with antibody.

### 2.4. Principle of detection

A schematic drawing illustrating the wireless nature of the magnetoelastic resonance biosensor and the basic principle for detecting bacterial cells is shown in Fig. 1.

As Fig. 1 denotes, the frequency spectrum of the sensor can be obtained by sweeping an AC magnetic interrogation field over a pre-determined frequency range while monitoring the response of the sensor using a pickup coil. At the resonance frequency of the sensor, the conversion of the magnetic energy into elastic energy is maximal and the sensor undergoes a magnetoelastic resonance. For a thin, ribbon-shaped sensor of length  $L$  vibrating in its basal plane the fundamental resonant frequency of the longitudinal vibrations is given by Plamen et al., 2000:

$$f = \sqrt{\frac{E}{\rho(1 - \sigma^2)}} \frac{1}{2L} \quad (1)$$

where  $E$  denotes Young's modulus of elasticity,  $\sigma$  is the Poisson ratio,  $\rho$  is the density of the sensor material, and  $L$  is the long dimension of the sensor. Due to the shape demagnetizing factors of the ribbon-like sensor, the magnetic permeability is greatest along its length. Hence an incident magnetic field will generate

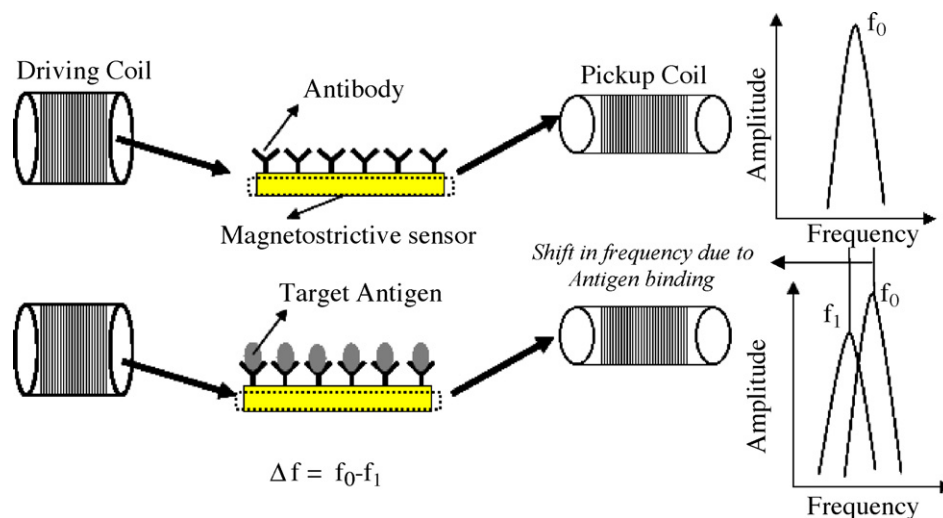


Fig. 1. Schematic drawing illustrating the wireless nature of the magnetoelastic resonance biosensor and the basic principle for detecting bacterial cells. The fundamental resonant frequency of the biosensor is  $f_0$  without antigen binding, which shifts (decreases) to  $f_1$  due to antigen binding to the antibody immobilized on the sensor surface.

longitudinal vibrations in the sensor from almost any orientation except normal to the basal plane of the sensor.

When testing temperature, humidity and other environmental parameters are invariable, a shift in resonance frequency of the magnetostrictive sensor depends only on the mass change ( $\Delta m$ ) on its surface. If the mass increase is small compared to the initial mass of the sensor the shift in the resonant frequency is given by (Cai et al., 2001)

$$\Delta f = -f \frac{\Delta m}{2M} \quad (2)$$

where  $f$  is the initial resonance frequency,  $M$  is the initial mass,  $\Delta m$  is the mass change, and  $\Delta f$  is the shift in the resonant frequency of the sensor.

Eq. (2) shows that the resonance frequency shifts linearly decreasing with increasing mass on the sensor surface. Hence binding of the target organism onto the biosensor surface causes a mass increase with a corresponding decrease in fundamental resonance frequency.

### 2.5. Bacteria binding measurements

After preparation of the biosensors, they were immersed in 1 ml solution of bacterial cultures for 30 min to bind bacterial cells and air-dried at room temperature. The resonance frequency of the sensors was measured using a HP network analyzer 8751A with S-parameter test set at 87511A before and after binding of bacterial cells to the immobilized antibody on the sensor. Each data point in all figures represents the mean of values obtained from six independent sensors, subjected to study under identical experimental conditions.

### 2.6. Microscopic analysis of sensors

Confirmation of antibody–bacteria binding at the sensor surface was conducted by scanning electron microscopy (SEM). Previously assayed biosensors were exposed to osmium tetra

oxide ( $\text{OsO}_4$ ) vapor for one hour to fix the bacterial cell wall to facilitate SEM observations. Then sensors were mounted onto aluminum stubs with carbon adhesive tape followed by gold (Au) sputtering (60 nm thickness) at 0.02 mbar argon (Ar) gas pressure to obtain a conductive surface for SEM imaging. The sensors were examined using a JSM-840 SEM, operating at 10 kV. The physical distribution and density of the bacterial cells attached to the sensor surface were examined.

## 3. Results and discussion

### 3.1. Response curves

The resonance frequency of the antibody immobilized magnetoelastic resonance sensors before and after binding *S. typhimurium* bacterium cells were measured. Fig. 2 shows the frequency spectrum obtained from a  $2 \text{ mm} \times 0.4 \text{ mm} \times 15 \mu\text{m}$  biosensor before and after exposure to a solution containing *S. typhimurium* at a concentration of  $1 \times 10^9$  CFU/ml. In this plot, the y-axis is the ratio of output voltage to input voltage, i.e. voltage amplitude. As can be seen that the voltage amplitude increases to a maximum at the resonance frequency and then decreases when passing the resonance frequency. The response obtained clearly shows that the resonance frequency decreases due to the binding of analyte (*S. typhimurium*) to the sensor surface. For these testing conditions a shift of 691 Hz was obtained.

### 3.2. Dose response

In order to investigate the role of the sensor size on the sensitivity of detection, sensors with different dimensions were prepared and used to detect solutions containing *S. typhimurium* with different known concentrations. Fig. 3 shows the resonant frequency shift for three different size sensors after exposure to solutions containing *S. typhimurium* bacteria with

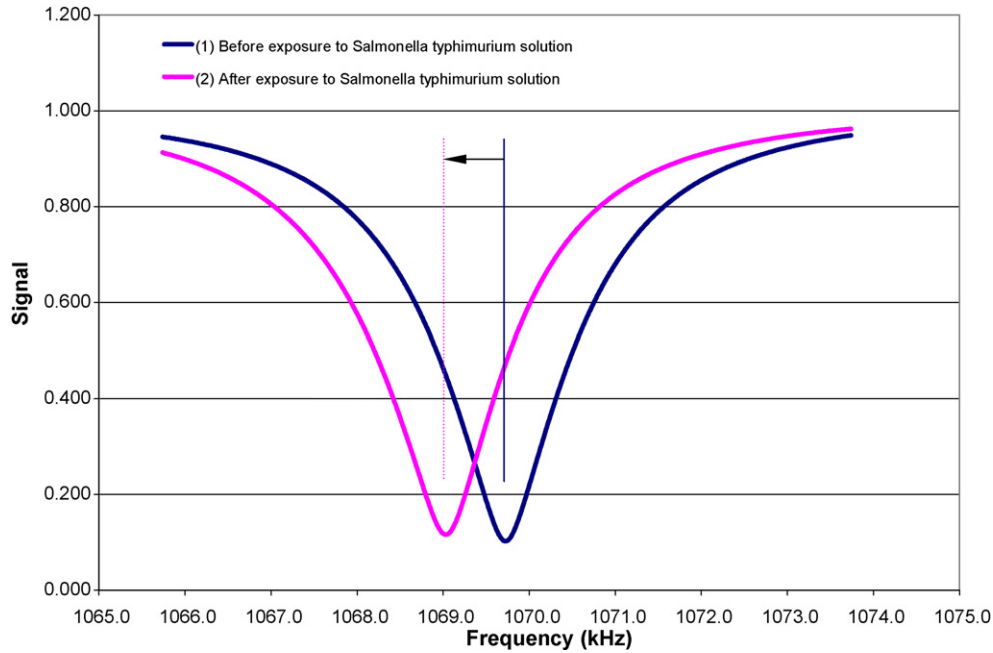


Fig. 2. Frequency spectrum of the antibody immobilized biosensor with the size of  $2\text{ mm} \times 0.4\text{ mm} \times 15\text{ }\mu\text{m}$ . The y-axis is the ratio of output voltage to input voltage which shows the relative output signal strength: (1) before exposure to *S. typhimurium* solution the resonant frequency  $f_0$  was 1,069,724 Hz; (2) after exposure to a solution containing *S. typhimurium* with a concentration of  $1 \times 10^9$  CFU/ml, the resonant frequency  $f_1$  decreased to 1,069,033 Hz. The resonant frequency shift  $\Delta f$  due to the binding of analyte (*S. typhimurium*) to the sensor surface:  $\Delta f = f_0 - f_1 = 1,069,724 - 1,069,033\text{ Hz} = 691\text{ Hz}$ .

different concentrations ranging from  $10^2$  to  $10^9$  CFU/ml. Fig. 3 also shows that the smaller the sensor size, the lower the detection limit, and the smaller the size, the bigger the resonant frequency shift for the same concentration. These observations are in good agreement with theory (Eq. (2)). From the responses obtained, it can be seen that the detection limit is  $5 \times 10^3$  CFU/ml,  $10^5$  CFU/ml and  $10^7$  CFU/ml for the sensors with the size of  $2\text{ mm} \times 0.4\text{ mm} \times 15\text{ }\mu\text{m}$ ,  $5\text{ mm} \times 1\text{ mm} \times 15\text{ }\mu\text{m}$  and  $25\text{ mm} \times 5\text{ mm} \times 15\text{ }\mu\text{m}$ , respectively.

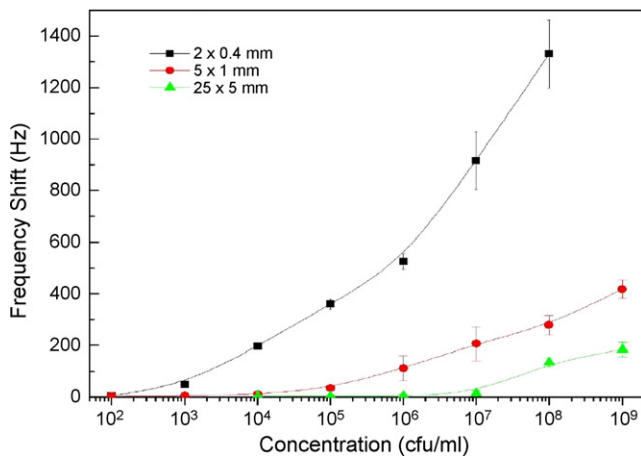


Fig. 3. The resonant frequency shift upon exposure to solutions containing *S. typhimurium* bacteria with different concentrations ranging from  $10^2$  to  $10^9$  CFU/ml for the  $15\text{ }\mu\text{m}$  thick sensors with the size: (1)  $2\text{ mm} \times 0.4\text{ mm}$ , (2)  $5\text{ mm} \times 1\text{ mm}$  and (3)  $25\text{ mm} \times 5\text{ mm}$ . The detection limit is  $5 \times 10^3$  CFU/ml,  $10^5$  CFU/ml and  $10^7$  CFU/ml for the sensors with the size of  $2\text{ mm} \times 0.4\text{ mm}$ ,  $5\text{ mm} \times 1\text{ mm}$  and  $25\text{ mm} \times 5\text{ mm}$ , respectively.

### 3.3. SEM observation

In order to confirm that the frequency shifts were mainly caused by the binding of *S. typhimurium* to the sensor's surface, SEM images were taken for the all sensors after exposure to bacterial solutions. Fig. 4(a)–(e) shows the typical SEM images of the biosensors with the size of  $5\text{ mm} \times 1\text{ mm}$  after exposure to different concentrations of *S. typhimurium* from  $10^9$  to  $10^5$  CFU/ml. The photos clearly show that exposure to decreasing concentrations of *S. typhimurium* led to a lower density of bound bacteria on the biosensor's surface and thus produced a smaller frequency shifts. The control sensor (Fig. 4(f)), with no antibody immobilized on its surface, when subjected to the highest concentration of  $10^9$  CFU/ml, had almost no binding of *S. typhimurium* cells. This confirms that the *S. typhimurium* cells bind specifically to the immobilized antibody, and that the antibody is immobilized on the sensor surface using the LB technique.

### 3.4. Correlation between SEM image and frequency shifts

Two different methods can be used to calculate the number of bacteria that have been captured on the surface of the magnetoelastic resonance biosensor. The first method is to calculate the area density of bacteria that attach to the sensor surface (bacteria attached per unit area) based upon the measured frequency shift of the biosensor. The second method is to directly count the number of bacteria attached to the sensor surface using SEM and statistically convert this to an area density of bacteria attached to the sensor surface. This section compares the results obtained using these two different methods.

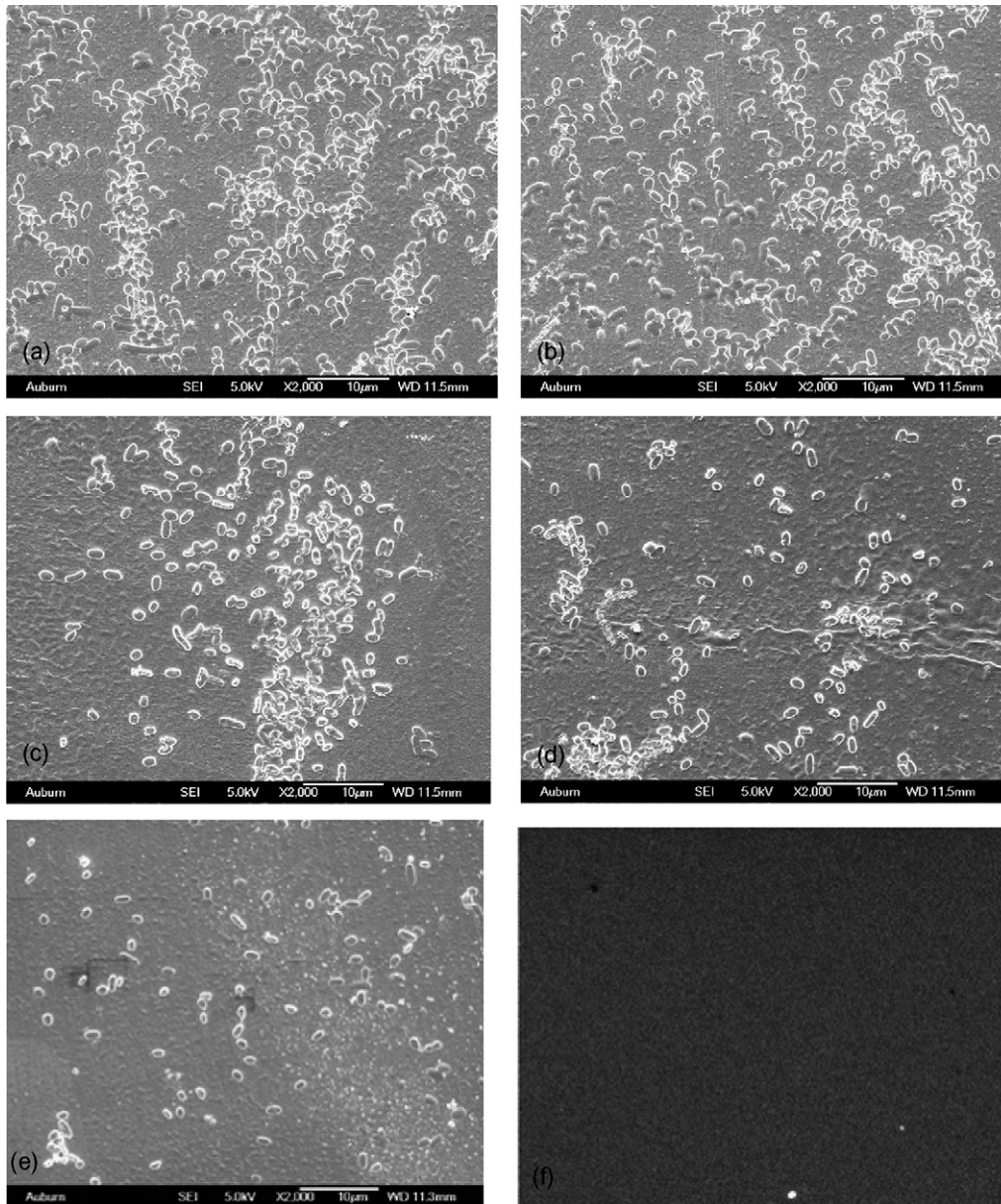


Fig. 4. (a)–(e) Typical SEM images of *S. typhimurium* bound to an antibody immobilized magnetoelastic resonance biosensor surface. Representative images of sensors exposed to solutions containing varying concentrations of bacteria (a)  $10^9$  CFU/ml, (b)  $10^8$  CFU/ml, (c)  $10^7$  CFU/ml, (d)  $10^6$  CFU/ml, (e)  $10^5$  CFU/ml. (f) Control sensor (devoid of antibody and exposed to  $10^9$  CFU/ml of bacterial solution).

#### 3.4.1. Calculation of bound bacteria density using measured frequency shift

During the testing process, the temperature, humidity and other related parameters are kept constant; therefore the resonant frequency shift is the result of an increase in mass due to the analyte (*S. typhimurium*) bound to the sensor surface. Since the increased mass is very small compared to the initial mass of the sensor, according to the measured resonant frequency shift,  $\Delta f$ , the additional mass,  $\Delta m$ , due to bacteria binding can be determined from the following Eq. (3) derived from Eq. (2).

$$\Delta m = -2\Delta f \frac{M}{f} \quad (3)$$

In our work, for the sensor with the dimensions of  $5 \text{ mm} \times 1 \text{ mm} \times 15 \text{ } \mu\text{m}$ , the fundamental resonance frequency can be determined according to Eq. (1). Using a Young's modulus value,  $E$ , of 110 GPa for the magnetostrictive material, a Poisson's ratio,  $\sigma$ , of approximately 0.3, and a magnetostrictive alloy density,  $\rho$ , of  $7.9 \text{ g/cm}^3$  (Magnetic Alloy 2826 Technical Bulletin, 2004) the calculated fundamental resonance frequency of the biosensor is 428 kHz. The sensor's natural mass (no bacteria attachment) was calculated to be  $5.925 \times 10^{-4} \text{ gm}$ . Thus, the additional mass  $\Delta m$  due to bacteria binding can be calculated from Eq. (3) and is

$$\Delta m = -2769\Delta f \quad (4)$$

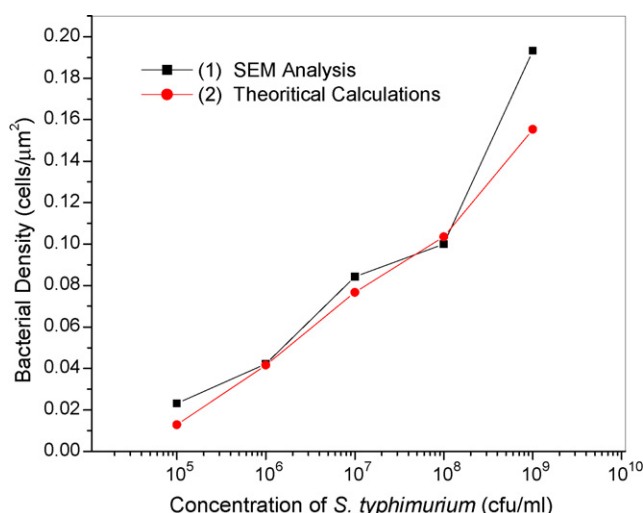


Fig. 5. Comparison of density of captured correlation of distribution of bacterial cells and the theoretically expected values for antibody immobilized sensors with the size of  $5 \text{ mm} \times 1 \text{ mm} \times 15 \text{ }\mu\text{m}$ . (1) The actual density of bacterial cells obtained from SEM images; (2) the theoretically expected density calculated from Eq. (5) according to the measured frequency shift.

where  $\Delta f$  is the frequency shift in Hz,  $\Delta m$  is the additional mass in pg.

Since the mass of each *S. typhimurium* cell is about 2 pg (Bailey, 2003), therefore, according to the calculated additional mass  $\Delta m$ , the number of *S. typhimurium* cells “ $n$ ” bound to the sensor’s surface can be theoretically determined as,

$$n = \frac{\Delta m}{2} \quad (5)$$

The density of *S. typhimurium* cells on the biosensor surface can then be calculated by dividing by the surface area of the sensor.

#### 3.4.2. Calculation of bound bacteria using SEM images

Ten different regions of each sensor surface were examined and photographed using SEM. The number of cells bound to the sensor surface was then measured and this number divided by the area of the surface examined. Fig. 5 compares the density of bacterial cells calculated based upon sensor frequency shift and the density of bacterial cells obtained from SEM images. Good agreement between the different calculation methods was obtained.

## 4. Conclusions

Polyclonal antibody immobilized magnetoelastic resonance biosensors were fabricated and their response to different concentrations of *S. typhimurium* bacteria was evaluated. The mass sensitivity of the biosensor increases with a decrease in the

sensor’s physical size. Detection limits of  $5 \times 10^3$  CFU/ml,  $10^5$  CFU/ml and  $10^7$  CFU/ml were obtained for  $15 \text{ }\mu\text{m}$  thick sensors with size of  $2 \text{ mm} \times 0.4 \text{ mm}$ ,  $5 \text{ mm} \times 1 \text{ mm}$  and  $25 \text{ mm} \times 5 \text{ mm}$ , respectively. SEM images provided visual verification that the measured frequency shifts were due to the attachment of bacteria to the sensor surface. Good agreement between the numbers of bound bacterial cells from SEM images and frequency shifts was obtained.

## Acknowledgements

This project was supported by USDA grant 2005-3439415674A.

## References

- Bailey, C.A., 2003. Ph.D. dissertation, Materials Engineering, Auburn University, Auburn, pp. 105–139.
- Bandey, H.L., Cernosek, R.W., Lee III, W.E., Ondrovic, L.E., 2004. Biosens. Bioelectron. 19, 1657–1665.
- Beckers, H.J., Tips, P.D., Soentoro, P.S.S., Delfgou-Van Asch, E.H.M., Peters, R., 1998. Food Microbiol. 5, 147–156.
- Gay, J., 1999. DVM PhD DACVPM, <http://www.vetmed.wsu.edu/courses-jmgay/FDIUHerdSalmonella.htm>.
- Cai, Q.Y., Jain, M.K., Grimes, C.A., 2001. Sens. Actuators B 77, 614–619.
- Committee for the National Institute for the Environment, 2005. Congressional Research Service, <http://www.cnre.org/nle/AgGlossary/letter-s.html>.
- Grimes, C.A., Kouzoudis, D., Mungle, C., 2000. Rev. Sci. Instrum. 71, 3822–3824.
- Howe, E., Harding, G., 2000. Biosens. Bioelectron. 15, 641–649.
- Hayes, P.S., Graves, L.M., Ajello, G.W., 1991. Appl. Environ. Microbiol. 57, 2109–2113.
- Jain, M.K., Schmidt, S., Ong, K.G., Mungle, C., Grimes, C.A., 2000. Smart Mater. Struct. 9, 502–510.
- Karpiskova, R., Pejchalova, M., Mokrosova, J., Vytrasova, J., Smuharova, P., Ruprich, J., 2000. J. Microbiol. Methods 41, 267–271.
- Ko, S., Grant, S.A., 2006. Biosens. Bioelectron. 21, 1283–1293.
- Kouzoudis, D., Grimes, C.A., 2000. J Appl. Phys. 87, 6301–6303.
- Luk, J.M.C., 1994. Biotechnology 17, 1038–1042.
- Magnetic Alloy 2826 (Iron nickel-based) Technical Bulletin, 2004, <http://www.metglas.com>.
- Oberst, R.D., Hays, M.P., Bohra, L.K., Phebus, R.K., Yamashiro, C.T., 1998. Appl. Environ. Microbiol. 64, 3389–3396.
- Oliveira, S.D., Santos, L.R., Schuch, D.M.T., Silva, A.B., Salle, C.T.P., Canal, C.W., 2002. Vet. Microbiol. 87, 25–35.
- Olsen, E.V., Pathirana, S.T., Samoylov, A.M., Barbaree, J.M., Chin, B.A., Neely, W.C., Vodyanoy, V., 2003. J. Microbiol. Methods 53, 273–285.
- Olsen, E.V., Sorokulova, I.B., Petrenko, V.A., Chen, I.H., Barbaree, J.M., Vitaly, J., Vodyanoy, V., 2006. Biosens. Bioelectron. 21, 1434–1442.
- Ong, K.G., Jain, M.K., Mungle, C., Schmidt, S., Grimes, C.A., 2001. SPIE 4467, 158–172.
- Pathirana, S.T., Vodyanoy, V., Barbaree, J.M., Chin, B.A., Hartell, M.G., Neely, W.C., 2000. Biosens. Bioelectron. 15, 135–141.
- Plamen, G., Stoyanov, P.G., Grimes, C.A., 2000. Sens. Actuators A Physical 80, 8–14.
- Rogers, K.R., 2006. Anal. Chim. 568, 222–231.
- Su, Xiao-Li, Li, Yanbin, 2005. Biosens. Bioelectron. 21, 840–848.
- Tims, T.B., Lim, D.V., 2004. J. Microbiol. Methods 59, 127–130.